Anisotropic intermediate valence in $Yb_2M_3Ga_9$ (M = Rh, Ir)

A. D. Christianson[1,2], J. M. Lawrence[1], A. M. Lobos[3], A. A. Aligia[3], E. D. Bauer[2], N. O. Moreno[2], C. H. Booth[4], E. A. Goremychkin[5], J. L. Sarrao[2], J. D. Thompson[2], C. D. Batista[2], F. R. Trouw[2], M. P. Hehlen[2]

[1]University of California Irvine, California, 92697, USA

[2]Los Alamos National Laboratory, Los Alamos, New Mexico, 87545, USA

[3]Centro Atómico Bariloche and Instituto Balseiro, Comisión Nacional de Energía Atómica, 8400 S. C. de Bariloche, Argentina

[4]Lawrence Berkeley National Laboratory, Berkeley California, 94550, USA

[5]Argonne National Laboratory, Argonne Illinois, 60439, USA

The intermediate valence compounds $Yb_2M_3Ga_9$ (M = Rh, Ir) exhibit an anisotropic magnetic susceptibility. We report measurements of the temperature dependence of the 4f occupation number, $n_f(T)$, for $Yb_2M_3Ga_9$ as well as the magnetic inelastic neutron scattering spectrum $S_{mag}(\Delta E)$ at 12 and 300 K for $Yb_2Rh_3Ga_9$. Both $n_f(T)$ and $S_{mag}(\Delta E)$ were calculated for the Anderson impurity model with crystal field terms within an approach based on the non-crossing approximation. These results corroborate the importance of crystal field effects in these materials; they also suggest that Anderson lattice effects are important to the physics of $Yb_2M_3Ga_9$.

PACS number(s): 75.30.Mb, 75.20.Hr, 71.27.+a, 71.28.+d

Most of the metallic intermediate valence (IV) compounds such as $CeSn_3$, $CePd_3$, and $YbAl_3$ are cubic and exhibit isotropic behavior. For these materials where the Kondo temperature is large ($T_K \geq 500K$) it is not necessary to invoke either magnetic RKKY interactions or crystal field (CF) effects to explain the physical behavior. Recently, Moreno *et al*.[1] have shown that CF interactions play an important role in the physics of the IV compounds $Yb_2M_3Ga_9$. This is manifested by a difference in the magnitudes, the Weiss constants and the temperatures of the maximum for the in-plane and out-of-plane magnetic susceptibility. The anisotropic susceptibility was reproduced by calculations using the Zwicknagl, Zevin and Fulde (ZZF) simplification[2] of the non-crossing approximation (NCA) to the Anderson impurity model (AIM), including the effects of CF interactions. (We note that the ZZF method for an AIM including crystal fields has been applied previously to the nearly-trivalent compound YbN.[3])

In this paper we report results for the temperature dependence of the 4f occupation number $n_f(T)$ for $Yb_2M_3Ga_9$ from 20 to 550 K measured using L_{III}-edge x-ray absorption[4] and also results of inelastic neutron scattering (INS) experiments[5] on polycrystalline samples of $Yb_2Rh_3Ga_9$ at 12 and 300 K. We compare the results of these measurements and of the earlier[1] measurements of the susceptibility $\chi(T)$ to the results of calculations based on the ZZF approach. We discuss the approximations involved and the role of Anderson *lattice* effects.

$Yb_2M_3Ga_9$ crystallize in a hexagonal structure (space group $P6_3cm$).[6] For the INS measurements, approximately 40 g of polycrystalline $Yb_2Rh_3Ga_9$ and $Y_2Rh_3Ga_9$ were

prepared by the following procedure. Stoichiometric amounts of Y and Rh were arc-melted together; the boule was flipped several times to ensure homogeneity. The resulting Y_2Rh_3 samples were placed in an alumina crucible with stoichiometric amounts of Ga and sealed in a silica tube under vacuum. In the case of $Yb_2Rh_3Ga_9$, stoichiometric amounts of Yb,Rh, and Ga were placed in an alumina crucible and sealed in a silica tube under vacuum. The samples were heated to 1150 °C, kept there for 1 hour, cooled to 1100 °C at a rate of 50 °C/hr, then cooled to 900 °C at a rate of 150 °C/hr, kept at 900 °C for 1-2 days, at which point the samples were quenched in liquid nitrogen. X-ray diffraction confirmed the hexagonal structure and magnetic susceptibility measurements were consistent with single crystal results. The resulting polycrystalline samples were then ground into powder and placed in a flat plate sample holder. Two time of flight chopper spectrometers were used: LRMECS at the Intense Pulsed Neutron Source (IPNS) at Argonne National Laboratory and PHAROS at the Los Alamos Neutron Science Center (LANSCE) at Los Alamos National Laboratory. The experimental configuration for these experiments was similar to that previously reported.[7 8] Incident energies, E_i, of 15, 35, and 120 meV were used on LRMECS at 12 and 300 K and 60 meV was used at 12 K. On PHAROS incident energies of 70 and 120 meV were used at 18 and 300 K.

The magnetic contribution to the INS spectrum (S_{mag}) was determined using a standard method,5[7] which assumes that the nonmagnetic scattering, (which dominates the scattering at large momentum transfer Q or high scattering angle) can be scaled to low angle (where the magnetic scattering dominates) in the same manner as observed experimentally in the nonmagnetic analogue compound $Y_2Rh_3Ga_9$. First, the data were

summed over scattering angle to create a low angle (LA) and a high angle (HA) bin with average angles of 20 and 90° respectively. Then the measured scattering from the nonmagnetic (NM) analog was used to determine a scaling factor R = S(NM, HA)/S(NM,LA), which was dependent on energy transfer ΔE and on E_i. This factor was then used to scale the high angle data to the low angle data of the Yb compound. Because of the differences in masses of Yb and Y and the resulting phonon frequency shifts we have not used a direct subtraction of the $Y_2Rh_3Ga_9$ data from the $Yb_2Rh_3Ga_9$ data (as in Ref. 8) to determine the magnetic contribution to the INS spectra.

For the L_{III} edge x-ray absorption measurements, single crystals were grown as in Ref. 1. These measurements were performed at beamline 4-3 of the Stanford Synchrotron Radiation Laboratory (SSRL) and were analyzed using standard procedures4 to obtain the temperature dependent 4f occupation number $n_f(T)$.

Fig. 1 displays minimally processed data (corrected only for counting time) collected for $Yb_2Rh_3Ga_9$ and $Y_2Rh_3Ga_9$. In (a) the temperature dependence of the low Q INS data collected on PHAROS with E_i = 120 meV for $Yb_2Rh_3Ga_9$ is shown. A noticeable decrease in the scattering for $40 < \Delta E < 90$ meV is observed in the 300 K data relative to that of the 18 K data. (The small feature at ~90 meV is an artifact of the empty holder scattering which has not been subtracted out.) In (b) the low Q INS data with E_i = 120 meV for $Yb_2Rh_3Ga_9$ collected on LRMECS (and corrected for sample mass, nuclear scattering cross-section, neutron absorption, and counting time, but not for the scattering of the empty sample holder) is compared to that for $Y_2Rh_3Ga_9$ at 12 and 300 K.

Magnetic scattering is evidenced by the stronger scattering in the Yb compound than in the Y compound. The scattering for $Y_2Rh_3Ga_9$ at 300 K is greater than for 12 K when $\Delta E < 30$meV, for which $n(\omega)+ 1$ is significantly greater than one where $n(\omega)$ is the Bose function; for larger ΔE the scattering is comparable at both 300 and 12 K. This type of temperature dependence is as expected for phonon scattering. In contrast, in$Yb_2Rh_3Ga_9$ the LRMECS data agrees with the PHAROS data in that the scattering at 300 K is actually *less* than at 12 K for $40 < \Delta E < 80$ meV. Hence, the temperature dependence can *not* be explained solely by the temperature dependence of phonon scattering but is as expected for CF excitations, where the occupation of the ground state multiplet decreases with temperature, and/or for the transfer of spectral weight from an inelastic response at low temperature to a quasielastic response at high temperatures.

Fig. 2 displays S_{mag} at 12 and 300 K for data collected on LRMECS for a variety of incident energies (in addition to the corrections listed for fig. 1(b) the contribution of the empty sample holder has been removed as well as the nonmagnetic background as described earlier). It can be seen clearly from the Lorentzian fits in Fig. 2(a) and (b) that the INS spectrum does indeed evolve from a high temperature quasielastic response to an inelastic response at low temperature. This is characteristic of IV systems[5]. At 12 K (Fig. 2(a)) the data can be fit with a single Lorentzian with width 27(1) meV and position 27(1) meV; at 300K (Fig. 2(b)) the data can be fit with a single Lorentzian centered at $\Delta E = 0$ meV (quasielastic) with width 20.7(4). Values of the static susceptibility can then be derived from these fits at 12 and 300 K and compared to the polycrystalline average of the measured static susceptibility (Fig. 2(c)). At 300 K the comparison is quite

reasonable, but at 12 K there is a discrepancy between the value of the static susceptibility derived from the INS results and those determined by the bulk measurements. Evidently, the INS measurements reported here are not sensitive to the low temperature upturn in the static susceptibility—neglecting this upturn results in more reasonable agreement. This suggests that the upturn is an extrinsic effect unless its contribution is only at low energies and thus not observable in these investigations.

The $n_f(T)$ results are displayed in Fig. 3. The data were collected over the temperature range from 20 to 550 K. The temperature dependence and magnitude of n_f is consistent with other Yb IV systems. The data indicate a somewhat higher degree of fractional valence in $Yb_2Ir_3Ga_9$ than in $Yb_2Rh_3Ga_9$.

We now turn to a discussion of systematic errors in our determination of S_{mag}. As discussed previously, we have used a standard procedure[5 7] to determine the nonmagnetic scattering. Specifically, we have used the nonmagnetic analog $Y_2Rh_3Ga_9$ to determine the scaling factor between the high and low angle data and then have applied that same scaling factor to the $Yb_2Rh_3Ga_9$ data. Systematic error could be introduced should the scaling factor depend significantly on the nuclear scattering cross section, which differs for Y and Yb. Since the magnetic susceptibility derived from the INS analysis compares favorably with that determined from bulk measurements, we argue that this has only a small (~10%) effect on our results. A small systematic error also could be introduced due to the strong neutron absorption in this material. We have minimized this by using a flat plat sample geometry, and correcting for the effects of neutron absorption.

Systematic error in the value of the 4f occupation number determined by L_{III} measurements is discussed in some detail in Ref. 4, where it is estimated to have an effect on the absolute value of n_f that is no larger than 5-10%. Such error should be independent of temperature and hence should not affect the temperature dependence determined for $n_f(T)$.

The AIM calculations that have been performed for the various experimental quantities shed additional light on the physics in the $Yb_2M_3Ga_9$ materials. These calculations are an extension of those reported in Ref. 1; for the INS calculations we used Eq. (39) of Zwicknagl et al.[2] with the same spectral density used in Ref. 1. In the lowest order calculation (parameter set 1, Table I) the CF splits the 8-fold degenerate ground state of Yb^{3+} into two quartets separated by the energy Δ. The CF wave functions are taken as eigenstates of the angular momentum operator J_z, where the ground state quartet consists of two doublets, $|\pm 7/2\rangle$ and $|\pm 5/2\rangle$, and the excited state quartet consists of the other two doublets, $|\pm 3/2\rangle$ and $|\pm 1/2\rangle$. This scheme gives a larger susceptibility for H//c than for H//a, due to the larger angular momentum (along the *c*-axis) in the ground state multiplet. By choosing the hybridization between the 4f and conduction electrons to have a value Γ = 165 K and the CF splitting to have a value Δ = 400 K, we reproduce the temperature of (~100 K) of the peak in $\chi_c(T)$, which arises from the Kondo effect (T_K = 194K) in a level of effective degeneracy four at low temperatures, and the temperature (~150 K) of the peak in $\chi_{ab}(T)$, which arises from the CF excitations. The fit to the susceptibility and 4f occupation number (dashed lines in Fig. 2(c) and lines in Fig. 3) is qualitatively quite

good. With the inclusion of a mean field interaction parameter I ($1/\chi_{tot} = 1/\chi_{NCA} + I$) this scheme gives excellent quantitative fits to the d.c. susceptibility (solid lines, Fig. 2(c)).

When calculating the INS spectrum the same mean field interaction parameter as used for the static susceptibility was included, as a reduction factor independent of energy. The fit to the INS (Fig. 2(a), dash-dot line) is of the right magnitude and overall energy scale, but shows two features, one at 20 meV representing the Kondo scattering in the ground state quartet and the other at 55 meV representing the CF excitation which due to the Kondo effect occurs at $k_B(\Delta + T_K)$. The fits to the INS can be improved (Fig. 2(a), dashed line) without affecting the susceptibility or occupation number by lifting the ground state degeneracy to two doublets separated by 7meV, lowering Δ to 340 K and allowing the hybridization constant Γ to be slightly different for the ground and excited multiplets (parameter set 2, Table I).

Overall, the combination of CF and Kondo physics gives good semi-quantitative fits to the anisotropic susceptibility, 4f occupation number and INS spectrum. In this sense, our calculations capture much of the essential physics of these compounds.

The ZZF approximation[2] ignores charge fluctuations such that only the spin fluctuations contribute to the susceptibility, as appropriate to the Kondo limit $n_f = 1$. Given the strong mixed valence of these compounds ($n_f \sim 0.6$) charge fluctuations will certainly contribute to the susceptibility. However, as shown by Bickers, Cox and Wilkins,[9] the susceptibility for $n_f = 0.7$ differs from the Kondo limit value by no more than 5%. We ignore this

difference because it is smaller than the amount that the susceptibility is reduced by inclusion of the molecular field parameter I = 25mol/emu (20% for χ_c and 10% for χ_{ab}). Such a parameter can arise due to antiferromagnetic interactions, but the Néel temperature T_N = 65K deduced from the formula $I = T_N / C_{7/2}$ (where $C_{7/2}$ = 2.58 emu-K/mol is the Yb Curie constant) is much larger than the ordering temperatures (~1K) seen in magnetic Yb compounds. It is reasonable to assert that the large value of I needed to improve the agreement between the magnitude of the measured susceptibility and the value calculated in the AIM is not due to normal RKKY interactions but is an Anderson *lattice* effect.

The existence of Anderson lattice effects is also suggested by the fact that our calculation significantly overestimates the 4f occupation number (Fig. 3) at 300K. Similar behavior of $n_f(T)$ in cubic IV compounds has been interpreted as evidence that the crossover from low temperature Fermi liquid behavior to high temperature local moment is *slower* in the Anderson lattice than in the AIM.[10] This effect arises primarily from the valence change that occurs as a function of temperature: for the Yb $4f^{14-nf}(5d6s)^{2+nf}$ configuration, $z = 2 + n_f(T)$ and Anderson/Kondo physics causes $n_f(T) \rightarrow 1$ for $T > T_K$, the Kondo temperature. For the Anderson lattice, a finite concentration of extra valence electrons $\Delta z = z(\infty) - z(0)$ must be accommodated by the conduction band. The resulting increase in kinetic energy is reduced by reducing the rate of the valence change with temperature, giving a "slow crossover." This is not the case for the AIM, where only one degree of freedom is involved.

The calculation of the INS at 300 K using parameter set 2 (the largest magnitude dashed curve in fig. 2(b)) also overestimates the data. We have calculated the neutron spectrum at 300 K using smaller values of $n_f(0)$ in parameter set 2 (Fig. 2(b)). By choosing the smaller T = 0 value $n_f(0) = 0.5$ that yields, in the context of the AIM, the actual experimental value of $n_f(300\ K) = 0.80$, we obtain much better agreement with $S_{mag}(\Delta E)$ at 300K and suggests that the slow crossover affects the temperature evolution of the dynamic susceptibility.

We have measured the temperature dependence of the 4f occupation number $n_f(T)$ of $Yb_2Rh_3Ga_9$ and $Yb_2Ir_3Ga_9$ as well as the INS response of $Yb_2Rh_3Ga_9$ at 12 and 300 K. The experimental results for $n_f(T)$ definitively establish that $Yb_2M_3Ga_9$ are IV systems. The INS spectra are similar to those seen in other IV systems, where the spectral weight shifts from a broad quasielastic response at high temperatures to a broadened inelastic response at low temperatures. We have performed AIM calculations which corroborate the results of Ref. 1 that crystal fields play an essential role in the physics of $Yb_2M_3Ga_9$ and that the AIM, with CF splitting, captures much of the essential physics. In addition, our results suggest that Anderson lattice effects must be considered to explain the temperature dependence of $n_f(T)$ and of the INS spectra; in particular, the temperature dependence suggests the presence of a slow crossover to the local moment regime.

Acknowledgements

Work at Irvine was supported by the Department of Energy (DOE) under Grant No. DE-FG03-03ER46036. Work at Los Alamos and Argonne was performed under the auspices

of the DOE. Work at Lawrence Berkeley National Laboratory was supported by the U.S. Department of Energy under Contract No. DE-AC03-76SF00098. Portions of this research were carried out at the Stanford Synchrotron Radiation Laboratory, a national user facility operated by Stanford University on behalf of the U.S. Department of Energy, Office of Basic Energy Sciences. This work was sponsored by PICT 03-12742 of ANPCyT. Two of us (A. L. and A. A. A.) are partially supported by CONICET.

Tables

	E(|±7/2⟩)	E(|±5/2⟩)	E(|±3/2⟩, |±1/2⟩)	$\Gamma_{\pm7/2,\pm5/2}$	$\Gamma_{\pm3/2,\pm1/2}$	I	T_K	γ	$n_f(0)$
$Yb_2Rh_3Ga_9$ 1	0	0	400	165	165	0	194	68 (45)	0.59
$Yb_2Rh_3Ga_9$ 2	0	80	340	180	170	25	280	66 (45)	0.60
$Yb_2Ir_3Ga_9$	0	0	280	230	230	45	1030	28 (25)	0.53

Table I: Fit parameters for NCA calculations for $Yb_2M_3Ga_9$. For $Yb_2Rh_3Ga_9$, 1 and 2 refer to parameter sets 1 and 2 as described in the text. The parameters for $Yb_2Ir_3Ga_9$ are from ref. 1 and have been included for comparison. The first three columns correspond to the energy of the CF levels, $\Gamma_{\pm7/2,\pm5/2}$ and $\Gamma_{\pm3/2,\pm1/2}$ denote the conduction electron hybridization to the specified CF levels, I is a mean field interaction parameter, T_K is the Kondo temperature, γ is the Sommerfeld parameter where the values in parentheses are experimental values from ref. 4, and $n_f(0)$ is the 4f occupation at T = 0 K. All units are in K except for I ((mol-Yb)/emu), γ (mJ/(mol Yb K^2)), and $n_f(0)$ (dimensionless).

Figure Captions

Fig. 1. (a) Comparison of data collected with PHAROS for $Yb_2Rh_3Ga_9$ at 18 (circles) and 300 K (squares) with E_i = 120 meV. (b) Comparison of data collected with LRMECS for $Yb_2Rh_3Ga_9$ and $Y_2Rh_3Ga_9$ with E_i = 120 meV. The squares (circles) denote the scattering for $Yb_2Rh_3Ga_9$ ($Y_2Rh_3Ga_9$) at 12 K. The solid (dashed) line denote the scattering for $Yb_2Rh_3Ga_9$ ($Y_2Rh_3Ga_9$) at 300 K. In both (a) and (b) the statistical errors bars are approximately the symbol size.

Fig. 2. Comparison of the magnetic part of INS data, S_{mag}, at 12 and 300 K and the magnetic susceptibility. (a) displays S_{mag} at 12 K with E_i = 15 (stars), 35 (circles), 60 (squares), and 120 (triangles) meV. The solid line is a Lorentzian fit with parameters as described in the text and the dash-dot (dashed) line is an AIM calculation for parameter set 1 (2) as described in the text. (b) displays S_{mag} at 300 K with E_i = 15 (stars), 35 (circles), and 120 (triangles) meV. The solid line is a Lorentzian fit with parameters as described in the text and the dashed lines are AIM calculations with parameters as described in the text. The upper most dashed curve corresponds to $n_f(0)$ = 0.6, the next lower $n_f(0)$ = 0.5, and the lowest $n_f(0)$ = 0.4. (c) displays the magnetic susceptibility for field applied along the c-axis (circles) and field applied in the basal plane (triangles) as well as the polycrystalline average (squares). The stars denote the values of the static susceptibility derived from

Lorentzian fits to the neutron scattering data at 12 and 300 K. The dashed (solid) lines denote AIM calculations of the static susceptibility for parameter sets 1 (2).

Fig. 3. $n_f(T)$ for $Yb_2Rh_3Ga_9$ (squares) and $Yb_2Ir_3Ga_9$ (triangles). Lines are AIM calculations as described in the text.

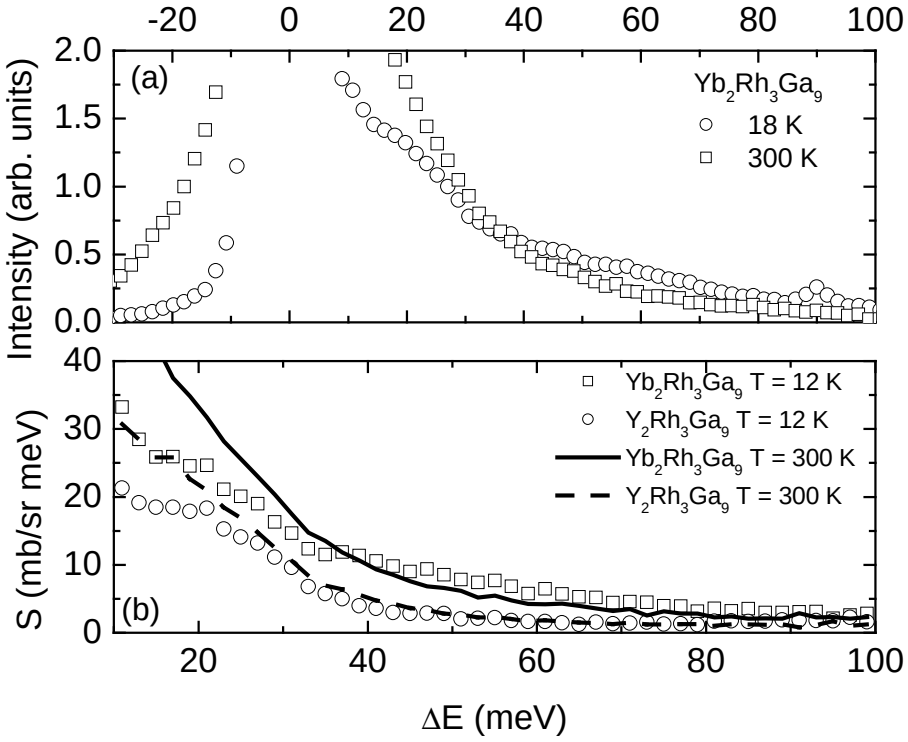
-20
0
20
40
60
80
100
2.0
1.5
1.0
0.5
0.0
Intensity (arb. units)
(a)
Yb2Rh3Ga9
18 K
300 K
40
30
20
10
0
S (mb/sr meV)
(b)
Yb2Rh3Ga9 T = 12 K
Y2Rh3Ga9 T = 12 K
Yb2Rh3Ga9 T = 300 K
Y2Rh3Ga9 T = 300 K
20
40
60
80
100
ΔE (meV)

Figure 1.

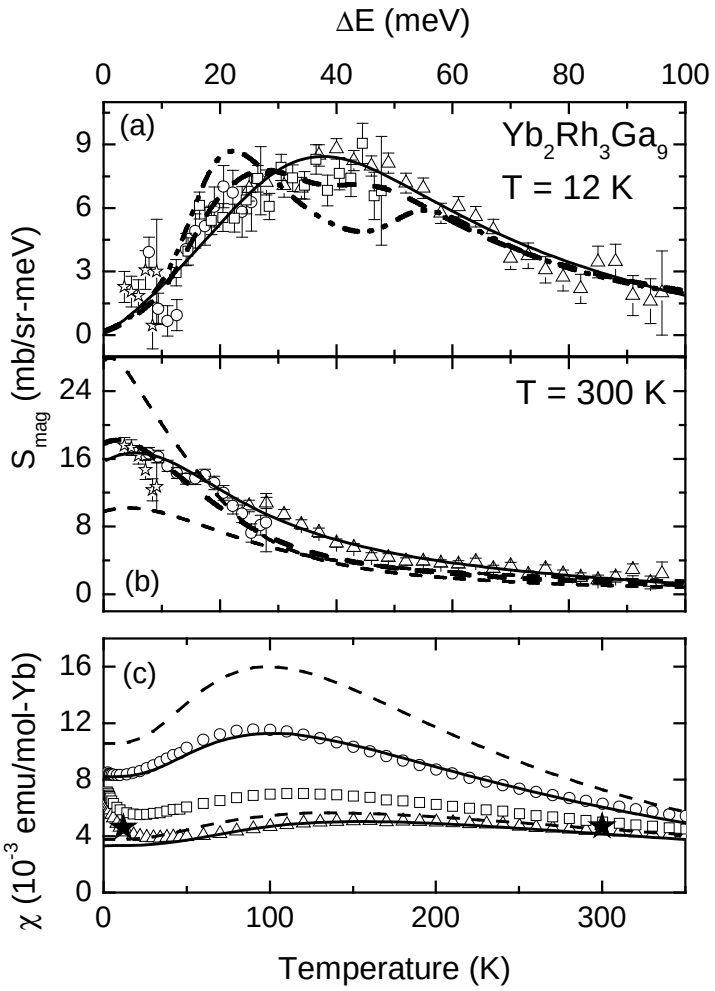
ΔE (meV)
0
20
40
60
80
100
(a)
Yb2Rh3Ga9
T = 12 K
9
6
3
0
T = 300 K
24
16
8
0
(b)
S_mag (mb/sr-meV)
(c)
16
12
8
4
0
χ (10^-3 emu/mol-Yb)
0
100
200
300
Temperature (K)

Figure 2.

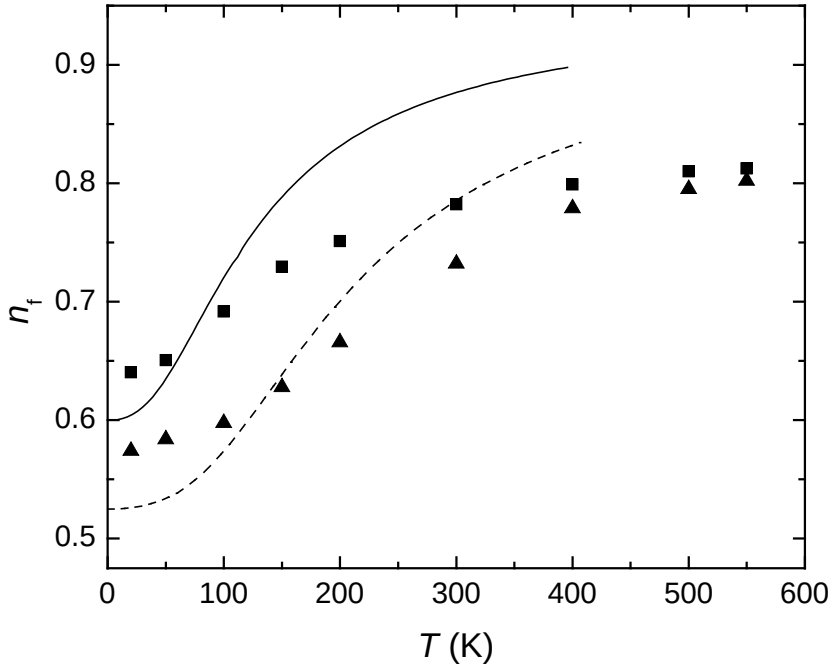

Figure 3.

[1] N. O. Moreno, A. Lobos, A. A. Aligia, E. D. Bauer, S. Bobev, V. Fritsch, J. L. Sarrao, P. G. Pagliuso, J. D. Thompson, C. D. Batista, and Z. Fisk, accepted to Phys. Rev. B, cond-mat/0502562.

[2] G. Zwicknagl, V. Zevin, and P. Fulde, Z. Phys. B: Condens. Matter **79**, 365 (1990).

[3] Yu. Zhou, S. P. Bowen, D. D. Koelling, and R. Monnier, Phys. Rev. B **43**, 11071 (1991).

[4] J. L. Sarrao, C. D, Immer, Z. Fisk Fisk, C. H. Booth, E. Figueroa, J. M. Lawrence, R. Modler, A. L. Cornelius, M. F. Hundley, G. H. Kwei, J. D. Thompson, and F. Bridges, Phys. Rev. B **59**, 6855 (1999).

[5] A. P. Murani, Phys. Rev. B **50**, 9882 (1994).

[6] S. Bobev *et al*., unpublished.

[7] J. M. Lawrence, R. Osborn, J. L. Sarrao, and Z. Fisk, Phys. Rev. B **59**, 1134 (1999).

[8] A. D. Christianson, E. D. Bauer, J. M. Lawrence, P. S. Riseborough, N. O. Moreno, P. G. Pagliuso, J. L. Sarrao, J. D. Thompson, E. A. Goremychkin, F. R. Trouw, M. P. Hehlen, and R. J. McQueeney, Phys. Rev. B **70**, 134505 (2004).

[9] N. E. Bickers, D. L. Cox, and J. W. Wilkins, Phys. Rev. B. **36**, 2036 (1987).

[10] J. M. Lawrence, P. S. Riseborough, C. H. Booth, J. L. Sarrao, J. D. Thompson, and R. Osborn, Phys. Rev. B **63**, 054427 (2001).